Growth and optical properties of $LiTm(WO_4)_2$ crystal

K.Kokh[1,2,*], A. Kraghzda[1,2], V. Svetlichnyu[3], E. Galashov[2], S. Raschenko[1,2], Yu. Seryotkin[1,2], A. Kuznetsov[1,2], A. Maillard[4], B. Uralbekov[5], A. Kokh[1]

[1]Sobolev Institute of Geology and Mineralogy, Novosibirsk, Russia
[2]Novosibirsk State University, Russia
[3]Siberian Physical–Technical Institute of Tomsk State University, Tomsk 634050, Russia
[4]Lorraine University and Supelec, Metz 57070, France
[5]al-Farabi Kazakh National University, Almaty 050000, Kazakhstan

*Corresponding author: Tel/Fax: +7 383 3066392, E-mail: kokh@igm.nsc.ru

Abstract

The bulk crystals of $LiTm(WO_4)_2$ were obtained by TSSG method from Li_2WO_4-WO_3 flux. Raman, luminescence and transmission spectra were obtained as well as crystal structure was refined by single x-ray measurements.

Keywords: double tungstates, crystal growth, structure, optical properties

Introduction

Much attention has been given in recent years to the study of tungstates family, especially of compounds containing rare earth elements. Their crystals were shown to be promising for laser[1], scintillator[2] and phosphor[3] applications. Single crystals of double tungstates of rare-earth and alkali elements are of special interest in laser industry.

In potassium containing matrices the active dopant concentration may be quite high without substantial fluorescence quenching because the inter-ion distance is large. For instance Yb-doped potassium-yttrium (KYW) and -gadolinium (KGW) crystals are the main compact media to generate ~1 μm femtosecond pulses [4]. Another promising host of Yb and Tm active ions is K-Lu double tungstate (KLuW) [5]. In case of Tm doping a laser generation in the two-micron range is achievable. Both Tm and Yb excitations are usually realized by commercial InGaAs and AlGaAs diode lasers.

In contrast to previous C2/c class of K-crystals, the sodium based rare earth tungstates represent tetragonal $I4_1/a$ symmetry and also may effectively host Yb. However in this structure mono- and trivalent cation positions are disordered which results in broadened absorption and fluorescence bandwidth [6]. Also some of the compounds like $NaY(WO_4)_2$ and $NaGd(WO_4)_2$ melt congruently, so may be grown in large size by Czochralski method [7].

Lithium has the smallest radius in the alkali metal series which turns to change of structural types in double tungstates. Heavy rare earth elements from La to Gd adopt tetragonal $I4_1/a$ structure. While the crystals with Tb-Lu including Y are monoclinic (P2/n) at room temperature [8], [9]. Some of the crystals of this family were obtained and characterized in terms of laser applications [10]; [11]; [12]; [13]. However no data exist on the LiTm tungstate except the early powder data of Klevtsova [8]. So in this work we were aimed to grow bulk $LiTm(WO_4)_2$ (LTW) crystal and to check its structural and optical properties.

Experimental

$TmNO_3$ (99.99%), WO_3 (99.99%), and Li_2CO_3 (99.999%) were used as starting reagents for the synthesis by solid-state reaction. After weighting the charge according to proportion 0,5 $TmNO_3$ + 0,5 Li_2CO_3 + 2WO_3, it was heated in air at 550 ^{0}C and kept at this temperature for 1 day.

Single crystal growth using Li_2WO_4-WO_3 flux was carried out by TSSG method. The platinum crucible with a diameter of 60 mm and 80 mm of height was used. In order to decrease volatilization of the components the crucible was covered by the cap. For crystal growth procedure the cooling rate and seed rotating speed were 0.5-0.7 deg/day and 1.2-2 rpm, correspondingly. After 2-4 weeks of growth, the crystal was pulled up and cooled at a rate of 15 deg/hour.

Thermal behavior in N_2 gas flow was investigated by DTA method using a NETZSCH STA 449F3 thermal analyzer. The heating/cooling rate was 15 ^{0}C/min.

X-ray diffraction data from single crystal were collected on an STOE IPDS2T diffractometer (image plate detector, graphite-monochromatized MoKα radiation) using ω-scan technique with scan width of 1° per frame. Diffraction signals were collected at room temperature with θ range from 2.0571 ° to 29.5565 °. Data reduction was performed with Oxford Diffraction CrysAlisPro software. SHELX-2014 software [14] in WinGX suite [15] was used for structure solution and refinement. Powder polycrystalline sample was studied on ARL X'TRA Bragg-Brentano diffractometer using Cu Kα radiation. The diffraction data were analyzed by the Rietveld method using FullProf software [16].

Vis- and IR absorption spectra of the sample were recorded using spectrophotometer Cary 100, Varian (operation range 200-900 nm, spectral resolution of 1 nm) and a FTIR spectrometer Tenzor 27, Bruker (375-7000 cm^{-1}, spectral resolution 4 cm^{-1}). Fluorescence was recorded by CM2203, SOLAR. Raman spectra were analyzed using a spectrometer InWia, Renishaw with excitation sources at 532 and 785 nm. All optical measurements were carried out at room temperature and with unpolarized light.

Result and discussion

X-ray powder diffraction data of the sample synthesized at 500°C are shown at Fig. 1a. The peaks correspond to the powder pattern of known double rare earth tungstates with lithium. The structure of LTW is not refined. Only unit cell parameters were published in [17], and our result is in agreement with that data. According to [8],[18] the compound melts at 1007°C and has polymorphic transitions I41/a->P2/c and further to P2/n at 976°C and 840°C, correspondingly. Thermal analysis of our sample shows one endothermic effect of melting at 1007°C. However there are two exo-peaks at 1000°C и 920°C (Fig.2). during the sample cooling. In order to exclude incongruent nature of LTW the sample was heated to 1100°C and then rapidly cooled to room temperature. Major lines of diffraction pattern of the sample (Fig. 1b) replicate that of synthesized monoclinic phase, while additional peaks (for instance at 2θ=29,34°) correspond well with tetragonal α-LTW [18] (Fig.1c). It may be concluded that the compound is likely to melt congruently and second peak at the cooling stage corresponds to the structural transformation from tetragonal to monoclinic phase. Thus it is necessary to use melt-solution to lower crystallization process below the phase transition temperature.

Solubility of LTW was studied in Li_2WO_4-WO_3 flux by modified visual polythermic technique [19] The flux was chosen as eutectic composition $0.45Li_2WO_4$+$0.55WO_3$ with melting temperature 744°C. Obtained results show that LTW has a wide region of primary crystallization in that flux (Fig.3). However due to intensive evaporation all experiments were conducted at LTW concentration <30 weight %.

First growth run using platinum wire resulted in the druse with plate-like grains around 0.5 mm thick (Fig.4a). Next the plates were used for seeded growth but monocrystal was not obtained. All experiments led to polycrystalline aggregate of parallel plates. This phenomenon may be explained by crystal splitting due to obstruction of crystallization front by flux components. Size of the plates was sufficiently increased by applying seed rotation during growth. As a result transparent grains with dimensions up to 10*15*3 mm were obtained (Fig.4c)

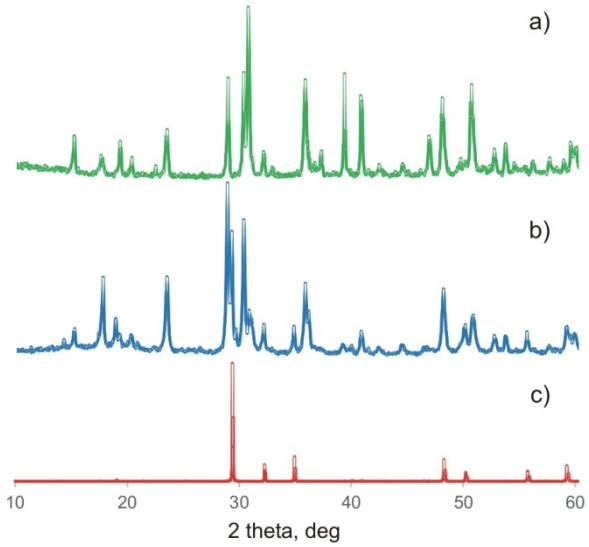

Fig.1. XRD pattern of $LiTm(WO_4)_2$: (a) as synthesized; (b) after quenching at 1100°C; (c) simulation of tetragonal α-modification [18].

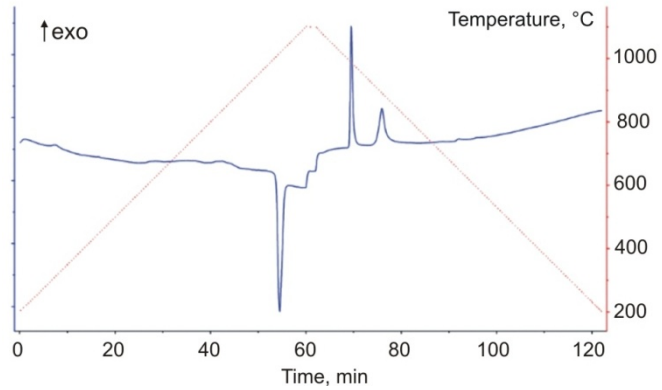

Fig.2. DSC curve of synthesized $LiTm(WO_4)_2$.

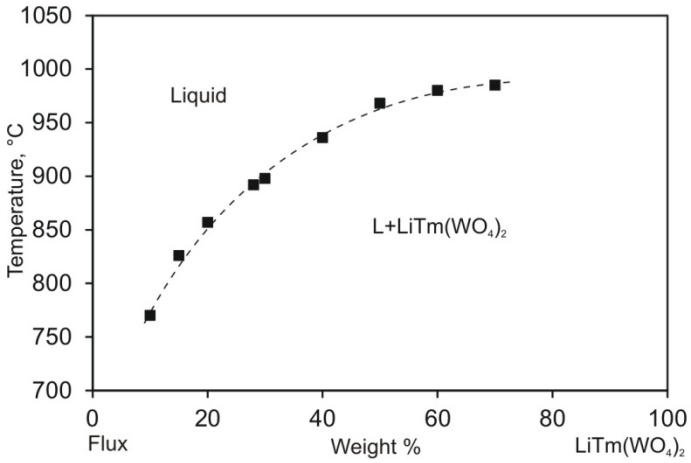

Fig. 3. Solubility curve of $LiTm(WO_4)_2$ in $0.45Li_2WO_4$+$0.55WO_3$ flux.

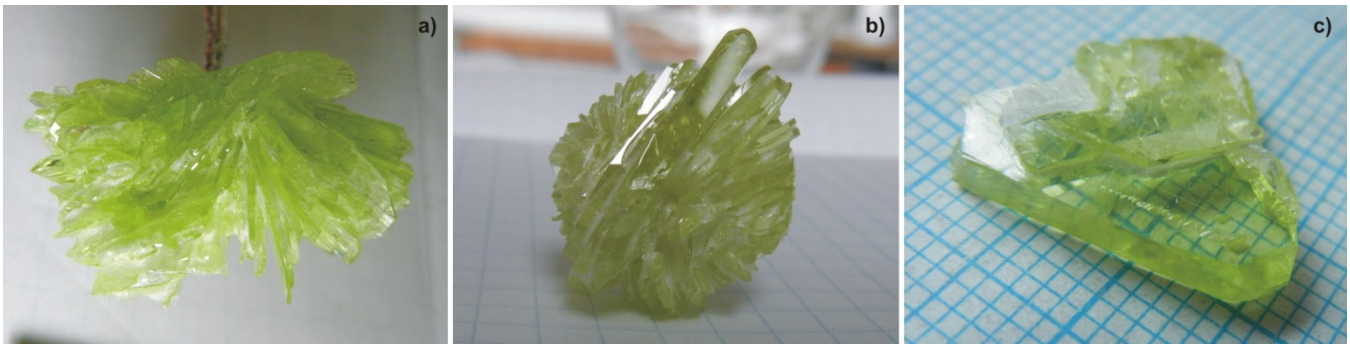

Fig. 4. $LiTm(WO_4)_2$ crystals: (a) spontaneously grown druse; (b) aggregate of parallel plates grown on seed; (c) transparent grain.

For crystal structure refinement a high quality single crystal with dimensions of 0.04 × 0.06 × 0.19 mm3 was selected using polarizing microscope. The details of data collection and structure refinement are summarized in Table 1. All structural data are listed in Table 2. Table 3 summarizes the interatomic distances.

The structure of LTW may be derived from that of wolframite $FeWO_4$ (P2/c) by the ordered replacement of Fe on Li and Tm atoms (Fig. 5a). Thus, the structure may be presented as alternating layers of zigzag chains composed of octahedrons WO_6 in one layer and LiO_6 + TmO_6 in another. The ordered Li and Tm arrangement leads to doubling of the corresponding cell and changes the symmetry plane type. The P2/n space group was selected for LTW as the most appropriate one on the basis of systematic absences and intensities of reflections.

However the use of refined structure parameters brings a considerable difference in the intensities of calculated diffraction peaks compared to experimental ones obtained from powder (Fig. 5b). It was assumed that the difference is caused by an effect of strong preferred orientation of grains in the sample, because wolframite mineral is known to have a perfect cleavage along {010}. In case of LTW a best fit was obtained by Rietveld refinement taking into account {351} (75.8 volume %) and {010} (40.5 volume %) directions (Fig. 5c).

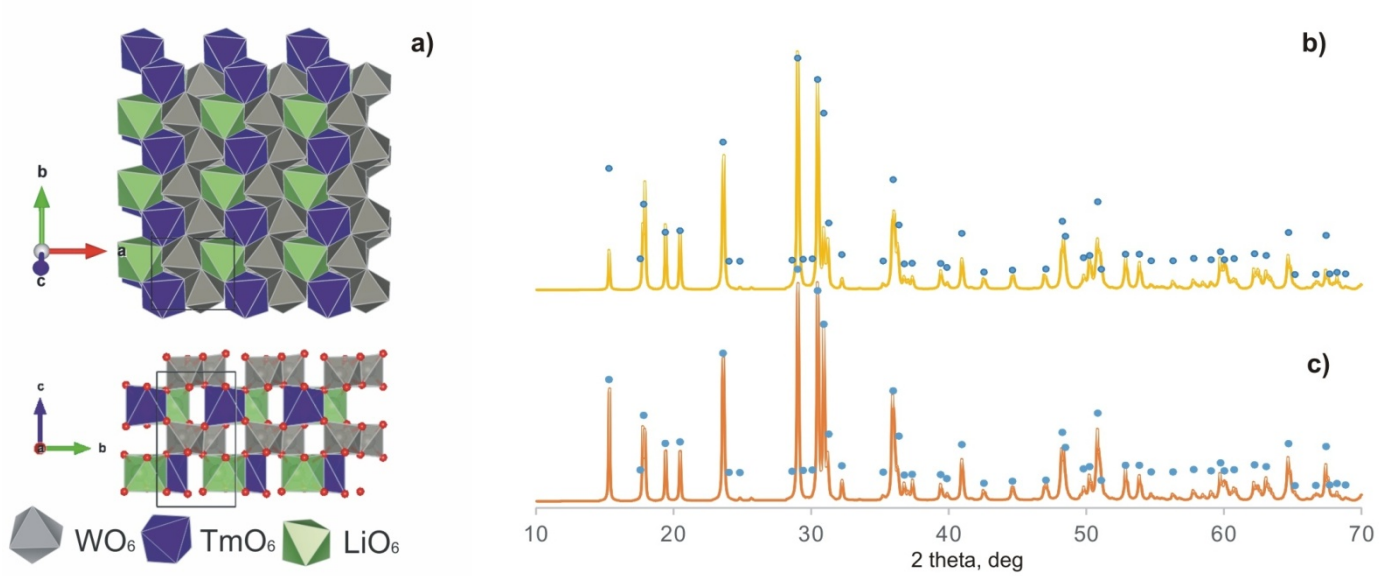

Fig.5. Crystal structure of $LiTm(WO_4)_2$ (a) and simulated powder XRD pattern without (b) and with (c) account of grain preffered orientation. Intensities of $LiTm(WO_4)_2$ experimental powder XRD are shown by circles.

Table 1. Parameters of Single-Crystal Data Collection and Structure Refinement

Formula	$LiTm(WO_4)_2$	
Formula weight	671.57	
Space group	P 2/n (No. 13)	P 2/c (No.13)*
a(Å)	4.99159(1)	9.9207(2)
b(Å)	5.78366(1)	5.7837(1)
c (Å)	9.92072(2)	10.8124(2)
B (^{o})	93.72180(2)	152.569(6)
V ($Å^3$)	285.806(10)	285.806(10)
Calculated density (g/cm^3)	7.804	
Absorption coefficient (mm^{-1})	55.536	
F(000)	568	
θ range (^{o})	2.0571-29.5565	
hkl limits	-6<h<6, -8<k<8, -13<l<13	
Measured reflections	8229	
Unique reflections	796	
Reflection with I>2δ(I)	783	
R_{int}	0.0833	
Refined parameters	54	
R factor (I>2δ(I))	R1=0.0354 wR2=0.1046	
R factor (all data)	R1=0.0360 wR2=0.1054	
Residual electron density(e/ $Å^3$)	Max= 5.942 min -3.951 av= 0.763	

* parameters for P2/c structure are presented for comparison

Table 2. Positional Parameters of $LiTm(WO_4)_2$ Structure

Atom	Wyckoff	x	y	z	Ueq
Li	2f	0.250000	-0.774(6)	-0.250000	0.021(6)
Tm	2e	0.250000	0.19809(9)	-0.750000	0.0095(2)
W	4g	0.224876(6)	-0.31831(6)	-0.51622(4)	0.0071(2)
O1	4g	0.093(12)	-0.1237(11)	-0.6353(6)	0.008(1)
O2	4g	0.3939(12)	-0.125(1)	-0.3901(6)	0.010(1)
O3	4g	0.4675(12)	-0.5861(11)	-0.3867(6)	0.011(1)
O4	4g	0.0513(12)	-0.6077(12)	-0.5961(6)	0.0095(11)

Atom	U_{11}	U_{22}	U_{33}	U_{23}	U_{13}	U_{12}
Tm	0.0125(3)	0.0093(3)	0.0070(3)	0	0.0023(2)	0
W	0.0066(2)	0.0077(3)	0.0071(3)	0.00064(1)	0.0008(1)	0.00024(8)
O1	0.011(3)	0.004(3)	0.010(3)	0.002(2)	-0.002(2)	-0.002(2)
O2	0.01(3)	0.010(3)	0.010(3)	-0.002(2)	0.001(2)	-0.002(2)
O3	0.011(2)	0.009(3)	0.013(2)	0.0014(2)	0.002(2)	0.004(2)
O4	0.011(2)	0.007(3)	0.011(3)	0.002(2)	0.003(2)	-0.001(2)

Table 3. Principal interatomic distances.

Atoms	Distance /Å
Li-O_1 (×2)	2.079(11)
Li-O_2 (×2)	2.59(2)
Li-O_3 (×2)	2.10(2)
Li-O Av.	2.25
W-O_1	1.774(6)
W-O_2	1.795(6)
W-O_3	1.848(6)
W-O_4	1.971(6)
W-O_4(x1)	2.073(6)
W-O_3(x1)	2.249(6)
W-O Av.	1.951
Tm-O_4(x2)	2.184(6)
Tm-O_2(x2)	2.224(6)
Tm-O_1(x2)	2.342(6)
Tm-O Av.	2.25

Absorption spectrum of LTW crystal plate is presented in Fig. 6. The short-wavelength absorption edge is positioned at ~300 nm, while in the range 350-2000 nm there are six absorption bands corresponded with transitions of Tm^{3+} ion from ground $^3H_6$ state to $^1D_2$, $^1G_4$, $^3F_3$, $^3H_4$, $^3H_5$, and $^3F_4$. Both structure and intensity of the bands may vary depending on thulium embedded matrix [20]; [21]; [22]; [23]. A wavelength range after 5 µm consists of vibrational absorption from ground $^3H_6$ state.

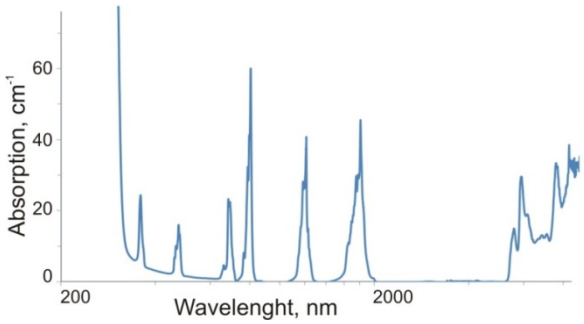

Fig.6. Absorption spectrum of $LiTm(WO_4)_2$.

Depending on the excitation wavelength, the crystal shows specific fluorescence of Tm^{3+} with most intensive lines at ~ 450 nm ($^1D_2 \rightarrow {}^3F_4$) and ~800 nm ($^3H_4 \rightarrow {}^3H_6$) [24] (Fig. 7a,b). Also a weak transition $^1G_4 \rightarrow {}^3F_4$ [24] was recorded at ~645 nm (Fig. 7c). It should be noted that excitation to $^1D_2$ state induces fluorescence of three above mentioned transitions, while $^1G_4 \rightarrow {}^3F_4$ and $^3H_4 \rightarrow {}^3H_6$ transitions are observed for excitation to $^1G_4$ state. It may be concluded that these states are interacted by relaxation processes. One of the specific thulium fluorescence line ($^3F_4 \rightarrow {}^3H_6$ transition) in the range 1.6-2.1 µm [25] is not shown. Apart from the Tm fluorescence, the excitation to total absorption band (below 300 nm) results in low intensity emission in the 360-460 nm range (Fig. 7d), which is likely to be a defect related luminescence.

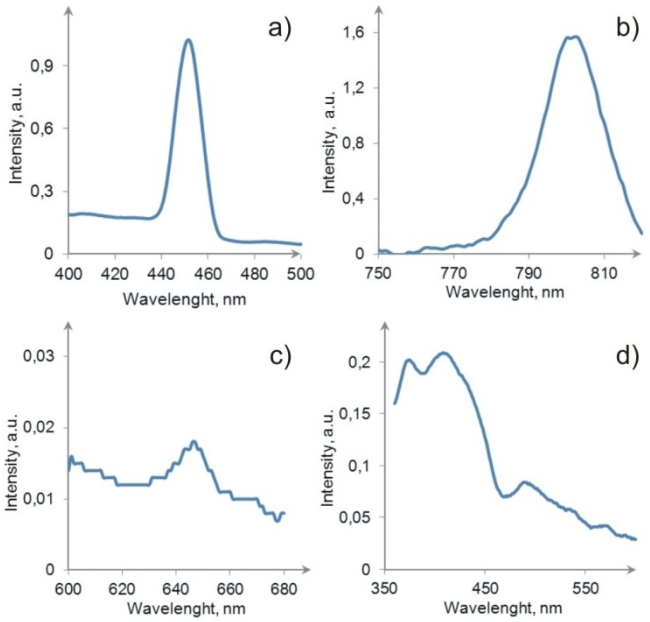

Fig. 7. Fluorescence spectra of $LiTm(WO_4)_2$.

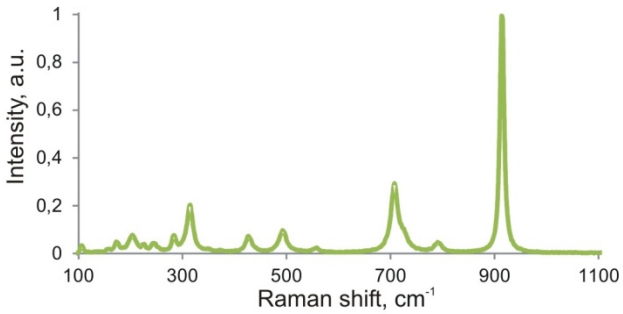

Fig. 8. Raman spectrum of $LiTm(WO_4)_2$.

The use of excitation source at 785 nm coincides with absorption band of $^3H_4$ state, so intensive emission at 810 nm (Fig. 7b) instead of Raman spectrum was obtained. Therefore 532 nm source was used to record Raman spectrum shown at Fig. 8. According to [26] a major intensities in the spectra are provided by the chains of distorted WO_6 octahedra. The bands between 490 and 710 cm^{-1} are supposed to be the effect of W_2O_2 bridge system vibrations. While the stretching and bending modes of WO_6 are located at higher and lower frequencies, correspondingly.

Conclusions

In this work a single crystal of $LiTm(WO_4)_2$ was obtained and characterized by basic optical methods. Tm ions demonstrated classical electron transitions, so the materials could be further studied in the scope of laser and luminescence applications. Comparison of structural parameters obtained by single crystal and powder XRD methods suggests the use of preferred orientation correction in the second case. This conclusion may also be concerned for other isostructural tungstates.

Acknowledgements

Thr research was supported by RSF grant #19-42-02003 in the part of crystal synthesis, project GF MES RK IRN AP05130794 and state assignment of IGM SB RAS

References:

(1) A.A. Kaminski, A.A. Pavlyuk, T.I. Butaeva, L.I. Bobovich, V.V. Lyubchenco, Neorg. Mater. 15 (1979) 541

(2) P. Lecoq, Development of new scintillators for medical applications // Nuclear Instruments and Methods in Physics Research Section A: Accelerators, Spectrometers, Detectors and Associated Equipment, 2016, 809, 130-139.

(3) M. Guzik, E. Tomaszewicz, S.M. Kaczmarek, J. Cybińska, H. Fuks. Spectroscopic investigations of $Cd_{0.25}Gd_{0.50}\square_{0.25}WO_4:Eu^{3+}$ — A new promising red phosphor // Journal of Non-Crystalline Solids, 356, (2010), 1902–1907

(4) G. H. Kim ; J. Yang ; D. S. Lee ; A. V. Kulik ; E. G. Sall' ; S. A. Chizhov ; V. E. Yashin ; U. Kang // Directly diode-pumped femtosecond laser based on an Yb:KYW crystal // Journal of Optical Technology c/c of Opticheskii Zhurnal 77(4):225-229 2010

(5) Valentin Petrov, Maria Cinta Pujol, Xavier Mateos, Oscar Silvestre, Simon Rivier, Magdalena Aguil´o, Rosa Maria Sol´e, Junhai Liu, Uwe Griebner, and Francesc D´ıaz. Growth and properties of KLu(WO4)2, and novel ytterbium and thulium lasers based on this monoclinic crystalline host // Laser & Photon. Rev. 1, No. 2, 179–212 (2007)

(6) J. H. Liu, V. Petrov, H. J. Zhang, J. Y. Wang, and M. H. Jiang, “Efficient passively Q-switched laser operation of Yb in the disordered NdGd(WO4)2 crystal host,” Opt. Lett. 32, 1728-1730 (2007).

(7) G.M. Kuz’micheva, D.A. Lis, K.A. Subbotin, V.B. Rybakov, E.V. Zharikov. Growth and structural X-ray investigations of scheelite-like single crystals Er, Ce:NaLa(MoO4)2 and Yb:NaGd(WO4)2 // Journal of Crystal Growth 275 (2005) e1835–e1842

(8) P. V. Klevtsov, C. P. Kozeeva, R. F. Klevtsova, N. A. Novgorodtseva "Preparation and Properties of Crystals of the $LiLn(WO_4)_2$ Double Tungstates for Ln = Rare Earth, Y, or Fe", all-union Symphosium on Crystal growth, Jubilee Meeting, 1969, page 107-109

(9) J.M. Postema, W.T.Fu, D.J.W.IJdo, Crystal structureofLiLnW2O8 (Ln¼lanthanidesandY): AnX-ray powder diffraction study // Journal of Solid State Chemistry 184, (2011) 2004–2008

(10) M. Derbal, D. Ouadjaout, F. Siserir, V. Jubera, J.P. Chaminade, A. Garcia, O. Viraphong, M. Kadi Hannifi. Emission spectrum and simulated laser parameters of Yb3+:LiLu(WO4)2 crystal // Optical Materials, 32 (2010) 756–758

(11) Xinyang Huang, Zhoubin Lin, Zushu Hu, Lizhen Zhang, Jingshun Huang, Guofu Wang. Growth, structure and spectroscopic characterizations of Nd3+-doped LiLa(WO4)2 crystal // Journal of Crystal Growth, 269 (2004) 401–407

(12) Xinyang Huang, Zhoubin Lin, Lizhen Zhang, Jiutong Chen, and Guofu Wang. Growth, Structure, and Spectral Characterization of LiNd(WO4)2 // Crystal growth & design, vol.6, no.10 2006 2271-2274

(13) Xinyang Huang, Guofu Wang. Growth and optical characteristics of Yb^{3+}:β-LiY(WO4)2 crystal // Optical Materials, 31 (2009) 919-922

(14) Sheldrick, G. M. Acta Crystallogr., Sect. A 2008, 64, 112−122.

(15) Farrugia, L. J. J. Appl. Crystallogr. 1999, 32, 837−838.

(16) Rodrı´guez-Carvajal, J. Recent advances in magnetic structure determination by neutron powder diffraction// Physica B: Condensed Matter Volume 192, Issues 1–2, October 1993, Pages 55-69

(17) Trunov V.K., Evdokimov A.A.: Double tungstates of lithium and rare earth elements. Soviet Physics Crystallography (translated from Kristallografiya) 19 (1975) 616-617

(18) Spitsyn V.I., Trunov V.K.: New data on double tungstates and molybdates of the MeLn(EO4)2 composition. Doklady Akademii Nauk SSSR 185(1969) 854-856
(19) Kononova N.G., Kokh A.E. RF Patent No. 2,195,520. Bul. No. 36, 27.12.2002.
(20) Lu Y., Dai Y., Wang J., Yang Y., Dong A., Li .S., Sun B. Spectra and intensity parameters of Tm3+ ion in YAlO3 crystal // Optics Communications 273 (2007) 182–186
(21) K. D. Knoll Absorption and Fluorescence Spectra of Tm3+i n YVO, and YPO // Phys. Stat. Sol. (b) 46, 553-559 (1971)
(22) Chrysochoos J. and Qusti A.H. Intense blue luminescence spectra and lifetimes of Tm(3+) IN POCl,:$SnCl_4$ // Journal of the Less-Common Metals, 126(1986) 161-167
(23) Zhekov V.I., Asatiani G.G., Melikishvili Z.G., Tsintsadze G.A., Sanadze T.I., Medoidze T.D., Petriashvili G.I., and Papashvili A.G. Absorption Spectra and Selective Excitation of Y3Al5O12: Tm3+ and YLiF4: Tm3+ Laser Systems // Laser Physics, Vol. 10, No. 2, 2000, pp. 532–539.
(24) Ryba-Romanowski W., Golab S., Sokolska I., Dominiak-Dzik G., Zawadzka J., Berkowski M., Fink-Finowicki J., Baba M. Spectroscopic characterization of a Tm3+:CSrGdGa3O7 crystal // Appl. Phys. B 68, 199–205 (1999)
(25) Lu Y., Dai Y., Wang J., Yang Y., Dong A., Li .S., Sun B. Spectra and intensity parameters of Tm3+ ion in YAlO3 crystal // Optics Communications 273 (2007) 182–186
(26) J. Hanuza, M. Maczka, and J.H van der Maas. Vibrational properties of double tungstates of the $M^{I}M^{III}(WO4)2$ family (M^{I}=Li,Na,K; M^{III}=Bi, Cr) // Journal of Solid State Chemistry, 117, 177-188, 1995